PHYSICAL REVIEW B **81**, 201403(R) (2010)

Atomic-resolution imaging of clean and hydrogen-terminated C(100)-(2×1) diamond surfaces using noncontact AFM

M. Nimmrich,[1] M. Kittelmann,[1] P. Rahe,[1] A. J. Mayne,[2] G. Dujardin,[2] A. von Schmidsfeld,[3] M. Reichling,[3] W. Harneit,[4] and A. Kühnle[1,*]

[1]*Institut für Physikalische Chemie, Fachbereich Chemie, Johannes Gutenberg-Universität Mainz, Jakob-Welder-Weg 11, 55099 Mainz, Germany*

[2]*Laboratoire de Photophysique Moléculaire, Université Paris-Sud, Bâtiment 210, 91405 Orsay Cedex, France*

[3]*Fachbereich Physik, Universität Osnabrück, Barbarastraße 7, 49076 Osnabrück, Germany*

[4]*Institut für Experimentalphysik, Freie Universität Berlin, Arnimallee 14, 14195 Berlin, Germany*

(Received 22 April 2010; published 14 May 2010)

High-purity, type IIa diamond is investigated by noncontact atomic force microscopy (NC-AFM). We present atomic-resolution images of both the electrically conducting hydrogen-terminated C(100)-(2×1):H surface and the insulating C(100)-(2×1) surface. For the hydrogen-terminated surface, a nearly square unit cell is imaged. In contrast to previous scanning tunneling microscopy experiments, NC-AFM imaging allows both hydrogen atoms within the unit cell to be resolved individually, indicating a symmetric dimer alignment. Upon removing the surface hydrogen, the diamond sample becomes insulating. We present atomic-resolution images, revealing individual C-C dimers. Our results provide real-space experimental evidence for a (2×1) dimer reconstruction of the truly insulating C(100) surface.

DOI: 10.1103/PhysRevB.81.201403 PACS number(s): 68.37.Ps, 61.66.Bi

Hydrogenated and clean diamond surfaces [see model in Figs. 1(a) and 1(b)] have attracted considerable interest in recent years, motivated by the unique electronic, thermal, mechanical, and optical properties of diamond,[1–3] which makes it suitable for high power laser and gyrotron applications or field-effect transistors.[4] Most of the diamond samples, both natural diamond and artificial chemical-vapor deposition (CVD) diamond, have a low impurity concentration and are insulating. For example, so-called type IIa diamond exhibits an impurity concentration of less than 1 ppm. Therefore, type IIa diamond is not sufficiently conducting for scanning tunneling microscopy (STM) imaging unless a water layer is present.[5,6] Thus, atomic force microscopy (AFM) appears to be the ideal tool for a high-resolution study of the diamond surface. Highest resolution has recently been demonstrated for bare dielectric surfaces[7–9] and molecules on insulators,[10–13] including submolecular resolution of a pentacene molecule at low temperature.[14] However, despite many attempts, atomic-scale AFM imaging of diamond surfaces has not been successful so far. To progress further in our understanding of diamond, a detailed characterization of its surface structure is necessary.

In this Rapid Communication, we present atomically resolved noncontact AFM (NC-AFM) images that reveal the individual hydrogen atoms on the hydrogenated diamond (100) surface, and the C-C dimers on the hydrogen-free diamond (100) surface. This is in contrast to high-resolution STM images of the hydrogenated diamond[6,15–18] and hydrogen-free diamond surfaces.[19–21] STM images of the hydrogenated diamond (100) surface could not separate the hydrogen atoms, which are clearly resolved in the NC-AFM image presented here. On the clean diamond (100) surface, individual C-C dimers could not be seen with the STM whereas they are clearly visible with the NC-AFM as demonstrated in this work. As a matter of fact, NC-AFM offers greatly enhanced resolution compared to STM for both the hydrogenated and clean diamond surfaces.

Experiments were performed at room temperature in an ultrahigh vacuum (UHV) system with a base pressure lower than 1×10^{-10} mbar. The system is equipped with a VT AFM 25 atomic force microscope (Omicron, Taunusstein, Germany) and an easyPLL Plus detector phase-locked loop detector and amplitude controller (Nanosurf, Liestal, Swit-

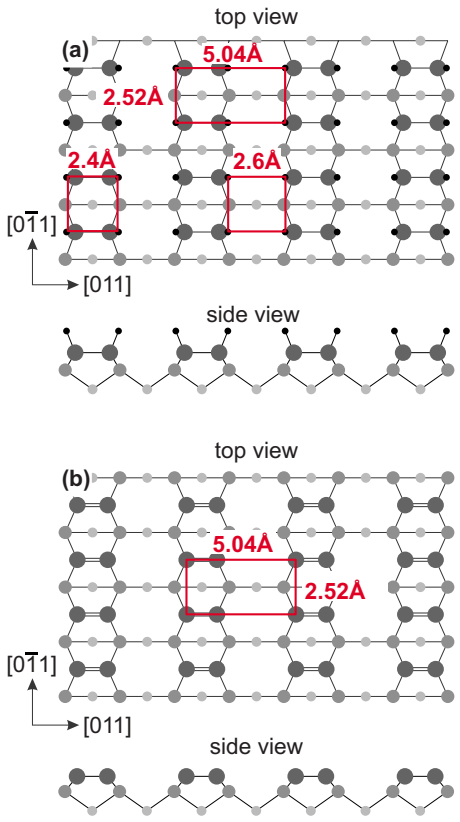

FIG. 1. (Color online) Model of the (a) hydrogen-terminated and (b) clean diamond (100)-(2×1) surface.

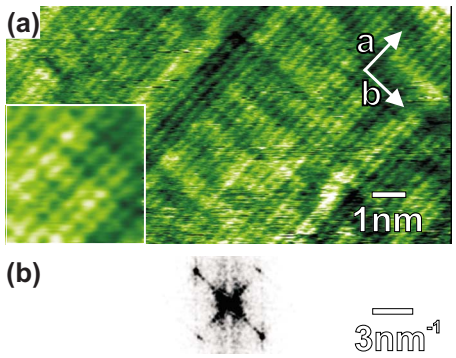

FIG. 2. (Color online) (a) NC-AFM frequency shift image of the hydrogen-terminated diamond C(100)-(2×1) surface (drift corrected raw data). To the lower left, a three-point mean filtered zoom (25 Å×25 Å) is added in order to show more clearly the atomic resolution. White arrows indicate the unit-cell directions. (b) 2D-FFT of the image shown in (a), revealing the unit-cell dimensions of $a=2.62\pm0.05$ Å and $b=2.53\pm0.04$ Å.

zerland) for oscillation excitation and signal demodulation. We use *n*-doped silicon cantilevers (NanoWorld, Neuchâtel, Switzerland) with resonance frequencies of about 300 kHz (type PPP-NCH), excited to oscillation with an amplitude of about 10 nm. Prior to their use, cantilevers were Ar^+ sputtered at 2 keV for 5 min to remove contaminants.

The type IIa CVD diamond samples of $3.0\times3.0\times0.5$ mm^3 in size were purchased from Diamond Detectors (Poole, U.K.). The samples are undoped. According to the supplier, the impurity concentration is below 1 ppm, with nitrogen being the largest portion. The investigated diamond (100) surfaces of the samples were etched and hydrogenated *ex situ* in a hydrogen plasma, as described in detail elsewhere.[22] The hydrogenated diamond samples were transferred into the UHV system and annealed to approximately 900 K for 1h to remove adsorbed contaminants from exposure to air, using a pyrolytic boron nitride radiation heater. This procedure is known to provide clean C(100)-(2×1):H surfaces.[17] The hydrogen can be removed by annealing the sample to a temperature of above 1200 K,[23] which was performed by heating the sample indirectly through a tantalum stripe mounted directly underneath the sample.

An NC-AFM image of the hydrogenated surface is shown in Fig. 2(a). The image represents raw data except for a drift correction that is applied as described elsewhere.[24] Figure 2(a) shows individual bright features, which are clearly visible in the enlarged view of a smaller area (25 Å×25 Å), forming the surface layer in an almost square arrangement. A two-dimensional fast Fourier transformation (2D-FFT) of the image was performed in order to determine the distance between protrusions [Fig. 2(b)]. As can be seen, the spacing between the topmost atoms, having dimensions of $a=2.62\pm0.05$ Å and $b=2.53\pm0.04$ Å, is nearly square.[25] These interatomic distances are in good agreement with previously published calculations of the diamond C(100)-(2×1):H surface structure, suggesting a hydrogen distance in the range of 2.58 Å (Refs. 26 and 27) to 2.62 Å (Ref. 28) in [011] direction and 2.52 Å (Refs. 28 and 29) in $[0\bar{1}1]$ direction, respectively.

These dimensions clearly indicate that our images resolve both hydrogen atoms within the unit cell individually, providing additional details to former STM measurements, which reveal electronic orbitals in between adjacent hydrogen atoms as bright dimers.[17] In the present image, faint modulations are visible, which can be ascribed to step edges. Note that a frequency shift image is shown that was taken with the height control loop operating with very low gains only. In such a case, the coarse height information is monitored in the topography channel while the fine corrugation is stored in the frequency shift channel. Hence, the corrugation measured in frequency shift images such as Fig. 2(a) does in general not represent the exact topography of the surface. The observed structure quality could be reproduced with another tip and matches the model expected from theory. Based on these experimental findings, the possibility of a multiple tip appears very unlikely to us. The present observation therefore confirms the monohydride model of the surface and indicates a symmetric C-C dimer alignment.

It is important to try to understand why we see the individual hydrogen atoms in AFM images and not in STM images where only the dimers are resolved. The key is that the STM is sensitive to the electronic structure whereas the AFM senses interaction forces. In a simple picture, the AFM is, therefore, sensitive to the spatial extension of the orbitals. In contrast, because of the applied bias, both the spatial extension and the position in energy of the different orbitals, with respect to the Fermi level, are important in STM. This may explain why the AFM probes the C-H bonds, whereas the STM favors the C-C surface states. Thus, the AFM offers the potential of providing further structural details in cases where the electronic structure is delocalized. However, detailed calculations will be necessary to fully understand this striking difference between NC-AFM and STM atomic-scale imaging of the hydrogenated C(100) surface.

Next, a hydrogenated sample was annealed to remove the chemisorbed hydrogen and to obtain a clean, insulating C(100)-(2×1) surface. NC-AFM topography images of the hydrogen-free surface are shown in Figs. 3(a) and 3(b). Besides drift correction, no further data processing was applied. Figure 3(a) displays terraces consisting of dimer rows. The dimer show a change in orientation of 90° between successive layers. The dimer-dimer distance within a row is $a'=2.50\pm0.05$ Å, the row distance is $b'=5.10\pm0.08$ Å. These distances are in good agreement with the unit-cell dimensions ($a'=2.52$ Å and $b'=5.04$ Å) of a (2×1) reconstruction, considering experimentally obtained bulk lattice dimensions.[29] Two different kinds of step edges are observed, namely, those aligned parallel to the direction of the dimer rows on the upper terrace [S_A (Ref. 30)] and those aligned perpendicular to the dimer rows (S_B), respectively. Figure 3(b) shows a terrace with single defects visible within the dimer rows, some of which are marked with white circles. Occasionally, multiple dimer vacancies aligned parallel to the dimer rows are observed, as marked with a white arrow in Fig. 3(b). Possible explanations for this might be hydrogen atoms remaining on the surface or missing C-C dimers. The types of defects most commonly found on all (100) oriented surfaces (such as Si, Ge, etc.) are either missing dimers or adsorbed species. In the case of diamond, this

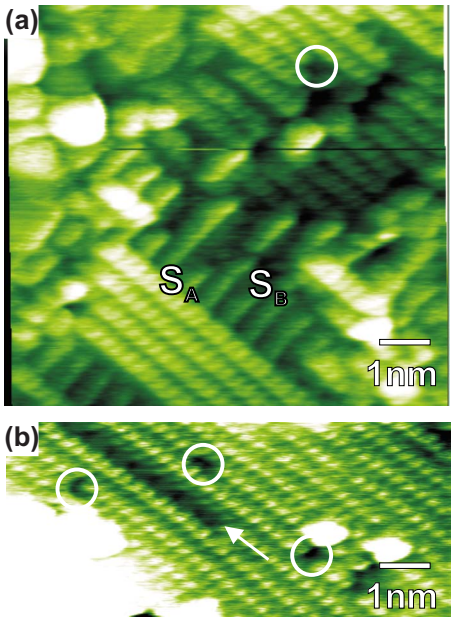

FIG. 3. (Color online) NC-AFM topography images of the clean diamond (100)-(2×1) surface (drift corrected raw data). (a) and (b) have been obtained at different measurement sessions using different tips.

would most likely be H, O, or CH_x.[17] Line defects are particular to the diamond surface because of the increased surface anisotropy driven by the differing stability of the two types of step risers.[16,17]

Although the samples studied are of highest quality available, the surface does still exhibit impurities, such as the larger aggregates to the left of Fig. 3(a). Nonaveraging, local imaging techniques such as NC-AFM are especially sensitive to impurities, even at very low concentration. In the case of diamond, a variety of different mechanisms may be causative for the observed impurities. Those impurities might originate from the bulk of the sample. For other elements, for example, bulk impurities are known to segregate to the surface, giving rise to a rather high density of surface impurities. Another option is that the impurities originate from the residual gas in the UHV chamber or are dropped from the tip during scanning. Both, adsorption from the residual gas and contamination by the tip, are well-known effects in scanning probe microscopy, even at very low background pressure and after sputtering the scanning probe tip.

Again, the AFM reveals the individual C-C dimers in each row, confirming the (2×1) surface reconstruction of undoped, truly insulating diamond. This is in contrast to the more uniform view of the dimer rows seen in the STM images on hydrogen-free CVD semiconducting diamond[21] or single-crystal insulating diamond.[20] In the latter STM study, a uniform one-dimensional density of states was observed due to the delocalization of the barrier resonances along the dimer rows. These barrier resonances are specific to the STM since they are created by the electric field between the STM tip and the surface.

In conclusion, we present high-resolution NC-AFM images of both, hydrogenated and clean, high-purity diamond (100) surfaces. In contrast to previously obtained STM images, we can resolve both hydrogen atoms in the unit cell of the C(100)-(2×1):H surface. Our NC-AFM images reveal atomic-resolution contrast on the clean, insulating diamond surface and provide real-space experimental evidence for a (2×1) surface reconstruction. This opens interesting perspectives for atomic-scale studies of molecular grafting on diamond surfaces. The much improved atomic-scale resolution of the NC-AFM, compared to the STM, confirms that NC-AFM is a unique probe of atomic-scale adsorbate and surface structures.

This work has been supported by the Volkswagen Stiftung through the program "Integration of molecular components in functional macroscopic systems."

*kuehnle@uni-mainz.de

[1] C. E. Nebel, Semicond. Sci. Technol. **18**, S1 (2003).
[2] J. E. Field, *The Properties of Natural and Synthetic Diamond* (Academic Press, London, 1992).
[3] S. Koizumi, C. E. Nebel, and M. Nesladek, *Physics and Applications of CVD Diamond* (Wiley-VCH, Weinheim, 2008).
[4] R. S. Balmer, J. Phys.: Condens. Matter **21**, 364221 (2009).
[5] F. Maier, M. Riedel, B. Mantel, J. Ristein, and L. Ley, Phys. Rev. Lett. **85**, 3472 (2000).
[6] L. Hellner, A. J. Mayne, R. Bernard, and G. Dujardin, Diamond Relat. Mater. **14**, 1529 (2005).
[7] R. Bechstein, C. González, J. Schütte, P. Jelínek, R. Pérez, and A. Kühnle, Nanotechnology **20**, 505703 (2009).
[8] S. Torbrügge, M. Reichling, A. Ishiyama, S. Morita, and Ó. Custance, Phys. Rev. Lett. **99**, 056101 (2007).
[9] S. Hirth, F. Ostendorf, and M. Reichling, Nanotechnology **17**, S148 (2006).
[10] S. A. Burke, J. M. Mativetsky, R. Hoffmann, and P. Grütter, Phys. Rev. Lett. **94**, 096102 (2005).
[11] T. Dienel, C. Loppacher, S. C. B. Mannsfeld, R. Forker, and T. Fritz, Adv. Mater. **20**, 959 (2008).
[12] S. Maier, L.-A. Fendt, L. Zimmerli, T. Glatzel, O. Pfeiffer, F. Diederich, and E. Meyer, Small **4**, 1115 (2008).
[13] P. Rahe, M. Nimmrich, A. Greuling, J. Schütte, I. G. Stará, J. Rybáček, G. Huerta-Angeles, I. Starý, M. Rohlfing, and A. Kühnle, J. Phys. Chem. C **114**, 1547 (2010).
[14] L. Gross, F. Mohn, N. Moll, P. Liljeroth, and G. Meyer, Science **325**, 1110 (2009).
[15] C. Nützenadel, O. M. Küttel, L. Diederich, E. Maillard-Schaller, O. Gröning, and L. Schlapbach, Surf. Sci. **369**, L111 (1996).
[16] K. Bobrov, A. J. Mayne, A. Hoffman, and G. Dujardin, Surf. Sci. **528**, 138 (2003).
[17] K. Bobrov, A. Mayne, G. Comtet, G. Dujardin, L. Hellner, and A. Hoffman, Phys. Rev. B **68**, 195416 (2003).
[18] R. E. Stallcup, A. F. Aviles, and J. M. Perez, Appl. Phys. Lett. **66**, 2331 (1995).

[19] R. E. Stallcup and J. M. Perez, Phys. Rev. Lett. **86**, 3368 (2001).
[20] K. Bobrov, A. J. Mayne, and G. Dujardin, Nature (London) **413**, 616 (2001).
[21] R. E. Stallcup and J. M. Perez, Appl. Phys. Lett. **81**, 4538 (2002).
[22] E. Tranvouez, E. Boer-Duchemin, A. J. Mayne, T. Vanderbruggen, M. Scheele, R. Cartwright, G. Comtet, G. Dujardin, O. Schneegans, and P. Chrètien, J. Appl. Phys. **106**, 054301 (2009).
[23] L. H. Chua, R. B. Jackman, J. S. Foord, P. R. Chalker, C. Johnston, and S. Romani, J. Vac. Sci. Technol. A **12**, 3033 (1994).
[24] P. Rahe, R. Bechstein, and A. Kühnle, J. Vac. Sci. Technol. B (to be published).
[25] The surface directions are rotated by 90° between successive layers. Because of the small difference in distance between adjacent hydrogen atoms in *a* and *b* directions, the spots caused by both types of layers in the 2D-FFT image superpose, resulting in broadened spots.
[26] D. R. Alfonso, D. A. Drabold, and S. E. Ulloa, Phys. Rev. B **51**, 14669 (1995).
[27] Y. Yu, C. Z. Gu, L. F. Xu, and S. B. Zhang, Phys. Rev. B **70**, 125423 (2004).
[28] S. H. Yang, D. A. Drabold, and J. B. Adams, Phys. Rev. B **48**, 5261 (1993).
[29] T. Hom, W. Kiszenick, and B. Post, J. Appl. Crystallogr. **8**, 457 (1975).
[30] D. J. Chadi, Phys. Rev. Lett. **59**, 1691 (1987).